A highly sensitive capacitive displacement sensor for force measurement integrated in an engineered heart tissue platform

Dostanic, M.; Pfaiffer, F.; Baghini, Mahdieh Shojaei; Windt, Laura; Wiendels, Maury; van Meer, Berend; Mummery, C. L.; Sarro, Pasqualina M; Mastrangeli, Massimo

Publication date
2023

Document Version
Accepted author manuscript

Published in
22nd International Conference on Solid-State Sensors, Actuators and Microsystems (TRANSDUCERS 2023)

Citation (APA)
Dostanic, M., Pfaiffer, F., Baghini, M. S., Windt, L., Wiendels, M., van Meer, B., Mummery, C. L., Sarro, P. M., & Mastrangeli, M. (2023). A highly sensitive capacitive displacement sensor for force measurement integrated in an engineered heart tissue platform. In *22nd International Conference on Solid-State Sensors, Actuators and Microsystems (TRANSDUCERS 2023)* (pp. 232-235). IEEE.

Important note
To cite this publication, please use the final published version (if applicable).
Please check the document version above.

A HIGHLY SENSITIVE CAPACITIVE DISPLACEMENT SENSOR FOR FORCE MEASUREMENT INTEGRATED IN AN ENGINEERED HEART TISSUE PLATFORM

Milica Dostanić[1,2], Filippo Pfaiffer[1], Mahdieh Shojaei-Baghini[1], Laura M. Windt[2], Maury Wiendels[2], Berend J. van Meer[2], Christine L. Mummery[2,3], Pasqualina M. Sarro[1] and Massimo Mastrangeli[1]

[1] Microelectronics, TU Delft, Delft, The Netherlands

[2] Anatomy and Embryology, LUMC, Leiden, The Netherlands

[3]Applied Stem Cell Technology, University of Twente, Enschede, The Netherlands

ABSTRACT

We present a novel capacitive displacement sensor integrated in an engineered heart tissue (EHT) platform to measure tissue contractile properties *in situ*. Co-planar spiral capacitors were integrated into the elastomeric substrate underneath the two micropillars of a previously developed EHT platform. The capacitor plates are displaced by the tension and compression that occurs in the substrate when the micropillars bend under contractile tissue force. For a contraction force of ~200 µN, applied in the middle of pillar length, the expected change in base capacitance is in the aF range. Readout of such low capacitance changes was achieved using a commercial low-noise high-sensitivity device. Characterization of static and dynamic sensor behavior agreed with numerical simulations, demonstrating a responsivity of 0.35 ± 0.07 fF/µN. Preliminary tests with cardiac tissues proved biocompatibility of the platform, as EHTs successfully formed and remained functional for at least 14 days.

KEYWORDS

Organ-on-chip, heart-on-chip, engineered heart tissue, microfabrication, capacitive sensing

INTRODUCTION

Engineered heart tissues (EHTs) have shown great potential in recapitulating organization, functions, and cell-cell interactions of the human heart *in vitro* [1]. EHTs result from the self-assembly of different cardiac cell types (e.g. myocytes and fibroblast) within an extracellular matrix (ECM) into tissues around two or multiple elastic anchoring points. After formation, EHTs begin contracting spontaneously, exerting force on the elastic micropillars. Contractile kinetics is a key hallmarks of cardiac function and hence a critical readout of EHT platforms. Currently, the contractile force is typically assessed by optically tracking the movement of elastic micropillars induced by the contracting tissues [2]. However, the procedure is laborious, and often cannot be conducted continuously and in real time. This limits the throughput and efficiency of the technology. Readout automation and high control of engineered microenvironments for EHT culture can therefore be achieved only by integrating force sensors within the platforms. An electrical force readout would allow precise real-time monitoring of the tissue contractile performance and enable closed-loop control systems for *e.g.* pacing and mechanical stimulation. Here we address these unmet needs by developing a co-planar capacitive displacement sensor for tissue contraction force measurement integrated within an EHT platform.

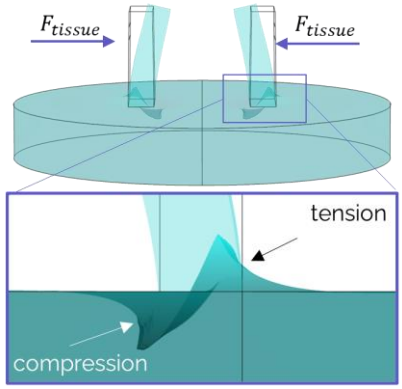

Figure 1. Illustration of micropillars bending upon tissue contraction in an elastomeric EHT platform, with close-up representation of the consequent substrate deformation. Magnitude of substrate deformation is amplified for the purpose of illustration.

DESIGN OF DISPLACEMENT SENSORS

The displacement sensors were incorporated into our previously developed polydimethylsiloxane (PDMS)-based EHT platform which featured two micropillars of rectangular cross-section within an elliptic microwell [3]. The pillar dimensions are 190 x 478 x 660 µm^3, while the elliptic microwell accommodates 3 µL of cell/ECM volume.

The working principle of the displacement sensors relies on deformation of the substrate in which the sensors are integrated. Bending of each micropillar caused by EHT contraction results in local anti-symmetric, out-of-plane deformation of the substrate (Fig. 1). This substrate deformation is captured by a pair of co-planar capacitive sensors consisting of two metal plates organized in a spiral geometry. Each metal plate interacts via fringing fields with its neighboring, oppositely charged plate. Substrate deformation affects the electric field line distribution between the metal plates, resulting in base capacitance change [4].

A pair of co-planar capacitive sensors integrated below each single micropillar results in a total of four sensors per EHT platform (Fig. 2A). Each of the capacitors is exposed to alternating compression and tension of the substrate, which enables the implementation of differential measurement of the base capacitance change. The spiral geometry selected maximizes sensitivity in the direction of the force applied by the tissue.

Four different spiral geometries with varying metallization ratios were designed and modeled in Comsol Multiphysics® to estimate base capacitance, sensitivity, and assess dynamic performance of sensors subject to tissue

contractile force. The top view of the platform with integrated sensors is shown in Fig. 2A with an individual spiral capacitor and relevant dimensions shown in Fig. 2B-C.

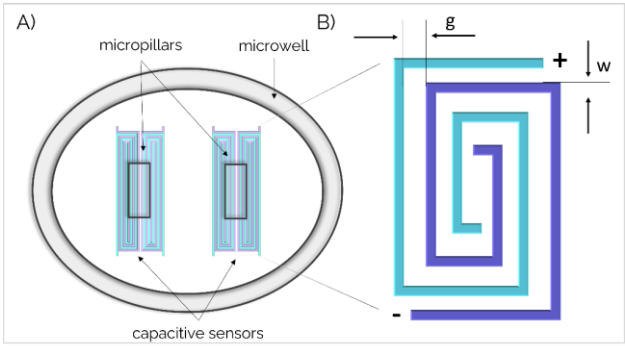

Sensor type	A	B	C	D
w [µm]	20	10	5	40
g [µm]	5	10	5	10

Figure 2. A) Top view of the EHT platform with two pairs of integrated capacitive sensors; B) A drawing of a single spiral capacitor with the relevant dimensions; C) Table with the dimension of all four types of sensors with varying metallization ratios.

CHIP FABRICATION AND ASSEMBLY

The sensors were integrated by means of an extended version of our established fabrication flow for the EHT platform using a combination of wafer-level micromachining and polymer processing (Fig. 3) [3].

Fabrication of the mould for micropillars and elliptic well started from plasma-enhanced chemical vapor deposition (PECVD) of a 5 µm-thick oxide layer on a single-side polished, 700 µm-thick Si wafer. The oxide layer was patterned using standard photolithography steps and dry etched to create a hard mask for deep reactive ion etching (DRIE) (Fig. 3A). After hard mask definition, DRIE of 660 µm-deep cavities in Si wafer followed. Prior to polydimethylsiloxane (PDMS) moulding, the Si surface was made hydrophobic by C_4F_8 deposition. The Si mould was finally covered with PDMS by two-step spin-coating to fill in the cavities in Si while obtaining a layer, less than 100 µm thick, on top of the wafer (Fig. 3B). The thickness of this layer determined the depth of integrated sensors. After the successful removal of PDMS structures from Si mould (Fig. 3C), contact openings were made in the PDMS layer with a circular biopsy puncher (1 mm in diameter) to later expose the contact pads for wire-bonding.

A second Si wafer was coated with C_4F_8 to obtain a hydrophobic surface prior to spin-coating an 80 µm-thick PDMS layer (Fig. 3D). Upon PDMS curing, degassing and surface activation in oxygen plasma, a 1 µm-thick layer of Al was sputtered at 25 °C and low power (1 kW) (Fig. 3E). The Al layer was patterned using standard photolithography techniques to obtain the four different spiral sensor designs across the wafer (Fig. 3F and 4A).

The final integration of sensors into the EHT platforms was performed by transferring PDMS structures from the Si mould and bonding them to the wafer with patterned Al lines. De-moulded PDMS structures were aligned to the patterned sensors using the surface tension of a water droplet on a transparent glass wafer (Fig. 3G). The two PDMS layers were bonded using uncured PDMS, followed by 1 hour of additional thermal curing. Single 10x10 mm^2 PDMS chips with integrated sensors were cut out and transferred to custom-designed printed circuit boards (PCBs). Chips were bonded to the PCBs using laser-cut pressure sensitive adhesive (PSA); and wire-bonds created an electrical connection between the Al pads patterned on PDMS and the contact pads on the PCB (Fig. 4B). Golden shims were attached using conductive glue on top of the Al contact pads to facilitate the wire-bonding. The shims provided mechanical support for the bonding process to avoid damaging the thin Al layer on PDMS due to the force applied during ultrasonic welding. Finally, acrylic wells (6 mm in diameter, 8 mm in height) were glued to the chips to contain the cell culturing medium (Fig. 4C). Additionally, all wire-bonds were insulated and encapsulated within PDMS. The assembly process resulted to be easily prone to failure due to the very critical wire-bonding and sensor transferring steps. Consequently, only two types of sensors (A and D) reached the end of the fabrication and packaging in the first fabrication iteration.

A highly-sensitive low-noise readout system was developed to detect the expected base capacitance change of the spiral co-planar capacitors in aF range. The readout system was based on the Analog Device AD7746, which per-

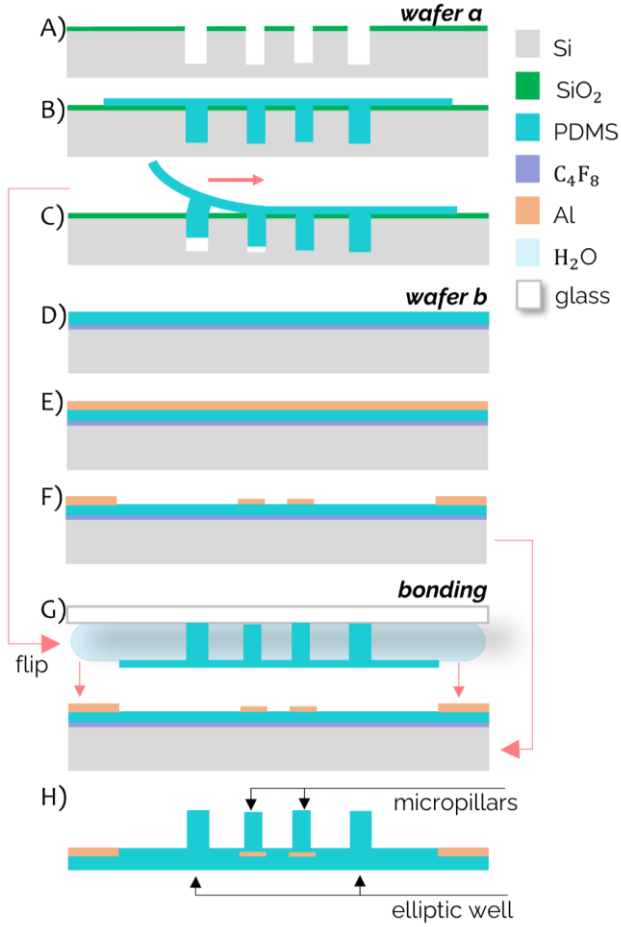

Figure 3. Sketch of the fabrication process of the PDMS-based EHT platform with integrated co-planar capacitive sensors: A-B) DRIE of tapered cavities into the Si mould; C)De-moulding of the PDMS structures; D-E) PDMS and Al deposition; F) Al photolithographic patterning; G) PDMS-mediated wafer bonding; H) released EHT platforms with integrated sensors.

forms capacitive-to-digital conversion using Σ-Δ modulation and enables low-noise, differential capacitive measurements [5]. The component has two capacitive channels, and each channel can be configured as single-ended or differential, enabling in total two differential measurements of two pairs of capacitors. The measurement range is ± 4.096 pF with 21-bit readout precision, achieving 4 aF resolution in the best case. The connection from single-chip PCB to the readout board was implemented with coaxial cables.

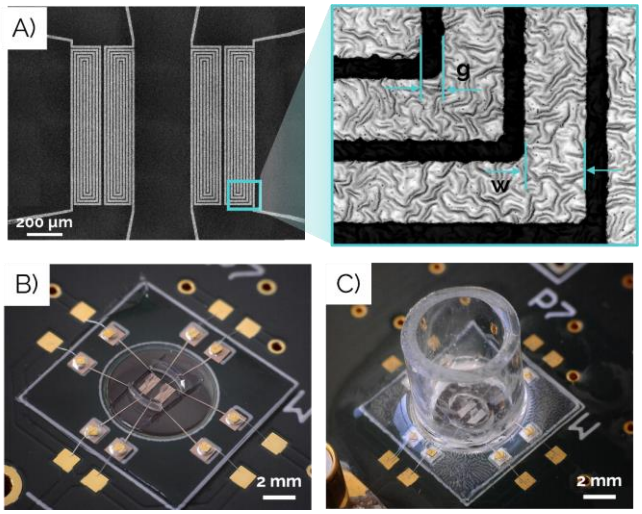

Figure 4. A) Optical image of the aluminum sensor type A patterned on top of a PDMS layer, with image of the 20µm-thick aluminum lines in the inset; B) Integrated capacitive sensor mounted and wire-bonded onto a custom-designed PCB; C) Packaging of the capacitive sensor, with the acrylic well for cell culture medium and wire-bonds encapsulation.

STATIC AND DYNAMIC ELECTRICAL CHARACTERIZATION

Electrical characterization of the sensors was performed by measuring the electrical output of sensors in both static and dynamic conditions. For sensor performance in static conditions, the base capacitance of the fabricated sensors was measured and compared to the values estimated from simulations. These measurements were performed using an Agilent 4294A Precision Impedance Analyzer connected to an electromagnetically shielded probe station (Cascade Microtech Summit 12k) with four independent sensing/force probes. Base capacitance was measured across the wafer for all four types of sensors. The measurements corresponded to the values obtained with FEM simulations and are shown in Table 1.

Table 1. Comparison of measured and simulated values of base capacitance for all four types of co-planar capacitive sensors.

Sensor type	A	B	C	D
Simulated value [fF]	374	279	497	231
Measured value [fF]	300±59	250±26	450±42	180±39

Dynamic characterization of the sensor behavior was performed using FemtoTools Nanomechanical Testing System (FT-NMT03). A silicon cantilever with flat circular tip, 50 µm in diameter, was used to apply force on different positions along the length of a micropillar, while measuring the electrical output of sensors. The single chip of a PDMS platform with integrated capacitive sensors was wire-bonded to a PCB custom-designed specifically for the nanoindentation purpose, and mounted on the metal holder (Fig. 5A). The Si probe movement was controlled via a micro-positioning stage connected to a PC. After mounting the PCB on the metal holder, the AD7746 readout system was connected to the PCB with coaxial cables, and the entire system was placed within a Faraday box to minimize environmental measurement noise. Measurements were performed by applying controlled force up to 300 µN on different positions along the micropillar length (Fig. 5B). Dynamic characterization was performed only for type D sensor, as it was the only sensor completing the entire assembly process. For the applied force in range of 100-300 µN, the measured capacitance change was 20-120 aF, resulting in responsivity of 0.35 ± 0.07 fF/µN. For the same applied force, the capacitance change is higher the closer the force is applied to the micropillar tip. The graph confirming the increase of the measured capacitance change with the increase in applied force is shown in Fig. 5C.

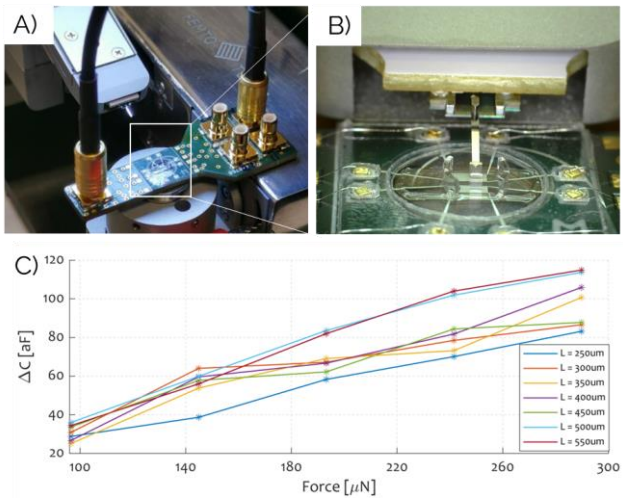

Figure 5. A) PCB with wire-bonded sensors mounted on the holder of the FemtoTool nanoindenter for characterization of dynamic sensor behavior; B) Close-up image of the nanoindenter silicon probe applying force along the micropillar length; C) Differential measurements of base capacitance change upon application of force on 7 different positions (denoted with L) along the length of a micropillar, obtained with the AD7746.

INCLUSION OF CARDIAC TISSUES

The assessment of the biocompatibility of the novel EHT platform with integrated co-planar capacitive displacement sensors was performed by culturing EHTs on the platform.

For the EHT formation, the same protocol was used as reported previously [6]. Briefly, three different cell types: cardiac fibroblasts (cFBs), cardiac endothelial cells (cECs) and cardiomyocytes (CMs) were derived from a human induced pluripotent stem cell (hiPSC) line (LUMC0020iCTRL-06). The hiPSCs were differentiated into cFBs, cECs and CMs as described previously [7]. The cell types were combined in a ratio of 70:15:15 of CMs, cFBs and cECs, respectively. For the ECM gel, 41% of acid solubilized collagen I (3.3 mg/mL), 5% of DMEM (10X), 6% of NaOH,9% of growth factor-reduced Matrigel and 39% of

formation medium was mixed. Next, the cell/ECM mixture was cultured in formation medium for 72h combined with VEGF (50 ng/mL) and FGF (5 ng/mL) to form EHTs. After 72h the culture medium was switched to BPEL + VEGF (50 ng/mL) + FGF (5 ng/mL) and maintained in culture for 14 days. The tissues successfully formed in both platforms with integrated sensors of type A and D. Representative images of tissues formed around the rectangular micropillars are shown in Fig. 6. Brightfield images were taken on day 8 since the beginning of the experiment with a Nikon Eclipse Ti2.

During the tissue culture experiments, the spontaneous force of contraction generated by the cardiomyocytes happened to be not high enough; therefore sensor efficiency for measuring contractile properties of EHT could not be tested, and is left as future work. Control tissues in standard platforms without sensors did not contract spontaneously either, indicating that in this first experiment, the cell batch used lacked normal functionality. Other cell culture features (e.g. formation and cell viability) seemed similar to control experiments. Therefore, biocompatibility of the platform was demonstrated, since the tissues remained viable in culture for 14 days.

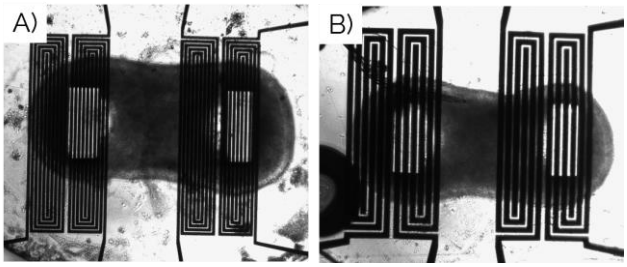

Figure 6. Formation of the EHTs in the platform with integrated sensors of type A (A) and type D (B).

CONCLUSIONS

We presented the design, fabrication and characterization of a novel, integrated capacitive co-planar displacement sensor for measurement of tissue contraction force in our previously developed EHT platform. The working principle of the sensor exploits the deformation in the elastomeric substrate occurring as a consequence of pillar displacement upon tissue contraction. Base capacitance change between co-planar metal plates upon their displacement was selected as the optimal sensing mechanism to estimate the force applied upon the micropillars, based on sensitivity and fabrication requirements. A pair of spiral capacitive co-planar sensors were positioned underneath each pillar in the areas of maximum substrate deformation, to measure both tension and compression occurring in the PDMS substrate. Four different spiral geometries were investigated and modeled using Comsol Multiphysics® to study the electrical response and sensitivity of sensors depending on the capacitor geometry.

Sensors were integrated into the EHT platform using a combination of silicon micromachining and polymer processing. All four sensor types were successfully patterned in 1 μm-thick Al layer and fabricated on a wafer level. However, it was shown that the assembly of the fabricated sensors into an experimental setup is challenging and prone to failures, and will be optimized in future versions of the devices. Consequently, only sensor type D was electrically characterized in dynamic conditions, while biological tests with EHTs were performed on sensor types A and D.

A readout system based on capacitive-to-digital conversion was developed to measure base capacitance change in the aF range, within a robust, low-noise and portable system. Analysis of system performance and sensitivity to noise proved the readout suitable for the intended capacitance measurements. The sensors that completed the assembly process were characterized by measuring their base capacitance, which showed good agreement with the values anticipated from simulations. The dynamic behavior of sensor type D was assessed using the nanoindentation setup by applying force up to 300 μN on different positions along the length of a micropillar. Based on these preliminary measurements, sensor responsivity was found to be 0.35 ± 0.07 fF/μN, setting the lower limit for the measurable tissue force with sensor type D at 100 μN.

Finally, the two assembled sensors were tested for biocompatibility by culturing EHTs for 14 days. Unfortunately, the tissues did not show expected spontaneous contraction and no force was visible by visual inspection nor detectable using the sensor. Repeated experiments will provide more insight into the feasibility of the developed sensors for real-time tissue contraction force monitoring.

ACKNOWLEDGEMENTS

The authors thank the staff of the Else Kooi Laboratory at TU Delft for their support in the fabrication of the devices. This work was supported by the Netherlands Organ-on-Chip Initiative (NOCI), an NWO Gravitation project (024.003.001).

REFERENCES

[1] J. M. Stein, C. L. Mummery, and M. Bellin, "Engineered models of the human heart: Directions and challenges," *Stem Cell Rep.*, vol. 16, no. 9, pp. 2049–2057, Sep. 2021.

[2] I. Mannhardt *et al.*, "A. Human Engineered Heart Tissue: Analysis of Contractile Force, " *Stem Cell Rep.*, vol. 7, no. 1, pp. 29-42, Jul 2016.

[3] M. Dostanić *et al.*, "A Miniaturized EHT Platform for Accurate Measurements of Tissue Contractile Properties," *J. Microelectromechanical Syst.*, vol. 29, no. 5, pp. 881–887, Oct. 2020.

[4] D. P. da Silva and S. F. Pichorim. "Modeling of Open Square Bifilar Planar Spiral Coils," *Journal of Microwaves, Optoelectronics and Electromagnetic Applications* vol.17, no. 3, pp. 319–339, Sept. 2018.

[5] F. Pfaiffer. "Towards a read-out for capacitive displacement sensor in an engineered heart tissue device," *MA thesis. 2022*

[6] A. Hansen *et al.*, "Development of a drug screening platform based on engineered heart tissue," *Circ. Res.*, vol. 107, no. 1, pp. 35–44, Jul. 2010.

[7] E. Giacomelli *et al.*, "Human-iPSC-Derived Cardiac Stromal Cells Enhance Maturation in 3D Cardiac Microtissues and Reveal Non-cardiomyocyte Contributions to Heart Disease," *Cell Stem Cell*, vol. 26, no. 6, pp. 862-879.e11, Jun. 2020.